ClearPotential: Learning the Dust-Corrected Potential of the Milky Way Using Flows

Eric Putney[1] **David Shih**[1] **Matthew R. Buckley**[1] **Sung Hak Lim**[2,1]
[1] NHETC, Department of Physics and Astronomy,
Rutgers, The State University of New Jersey, Piscataway, New Jersey 08854, USA
[2]Particle Theory and Cosmology Group, Center for Theoretical Physics of the Universe,
Institute for Basic Science (IBS), Yuseong-gu, Daejeon 34126, Republic of Korea
eputney,shih,mbuckley@physics.rutgers.edu
sunghak.lim@ibs.re.kr

Abstract

We introduce ClearPotential, a data-driven and dust-corrected measurement of the local Milky Way's gravitational potential using unsupervised machine learning, without the symmetry assumptions, specific functional forms, and binning required in previous work. The potential is modeled as a neural network, optimized to solve the equilibrium collisionless Boltzmann equation for the observed phase space density of *Gaia* DR3 Red Clump and Red Giant Branch stars within 4 kpc of the Sun. This density is obtained from data using normalizing flows, and our unsupervised solution to the Boltzmann equation automatically corrects for selection effects from crowding and the dust-driven extinction of starlight. Our fully-differentiable and unbinned machine learning model of the gravitational potential allows us to compute the acceleration and mass density, providing a three-dimensional map of the dark matter density in our local Galaxy. This work provides the clearest map of the local Galactic potential to date and marks an important step in the era of data-driven astrometry.

1 Introduction

Although we do not yet understand the particle nature of dark matter, both astronomy and cosmology provide a wealth of evidence for how dark matter evolves and clusters at various scales [1–19]. At galactic scales, dark matter forms into halos – massive gravitational basins that allowed for the rapid formation of visible baryonic structure – which dictate the evolution of stellar kinematics in galaxies such as our own Milky Way. The strong gravitational signature of our halo provides a local "laboratory" that allows us to place constraints on the underlying particle properties of dark matter.

One method for probing the gravitational potential sourced by our halo is through solving the *collisionless Boltzmann equation* (CBE). In the context of the CBE, stars are tracer particles of a collisionless fluid described by a time-dependent phase space density $f(\vec{x}, \vec{v}, t)$ of position $\vec{x}$ and velocity $\vec{v}$, which evolves in response to a potential sourced by dark matter, gas, and stars:

$$\frac{\partial f}{\partial t} + \vec{v} \cdot \frac{\partial f}{\partial \vec{x}} - \frac{\partial \Phi}{\partial \vec{x}} \cdot \frac{\partial f}{\partial \vec{v}} = 0. \tag{1}$$

In standard galactic dynamics, the potential Φ is recovered from the CBE by solving it in the equilibrium (stationary) limit where $\partial_t f = 0$. While recent studies using astrometric data from the *Gaia* space observatory have uncovered a range of disequilibrium features in the Milky Way Galaxy [20–32], this disequilibrium term is neither straightforward to compute nor is its impact on solutions

Machine Learning and the Physical Sciences Workshop, NeurIPS 2025.

of the CBE understood. Therefore, CBE-based studies select older, more equilibrated populations to mitigate the effects of this term.

Due to the limited size of previous astrometric datasets, traditional approaches instead solve velocity moments of the CBE, requiring simplifying assumptions about the parametric form or symmetries respected by both Φ and f [33–38]. However, in the era of *Gaia* astrometry these assumptions may potentially neglect significant amounts of kinematic information in our Galactic system. In this work, we solve the full six-dimensional equilibrium CBE in a completely data-driven way – without assuming underlying symmetries or parametric forms – using normalizing flows for an unsupervised machine learning approach to density estimation.

Given a flow-based estimate of f, we have immediate access to the density derivatives $\partial_{\vec{x}} f$ and $\partial_{\vec{v}} f$ across the six-dimensional phase space. Solving the CBE – a scalar equation – at a single location requires solving a system of at least three equations, each with unique velocities $\vec{v}$. In order to select at least three unique $(\vec{x}, \vec{v})$ pairs that have support under f (to guarantee accurate gradients), we factorize the phase space density into two functions $f(\vec{x}, \vec{v}) = n(\vec{x})p(\vec{v}|\vec{x})$, the number density and conditional velocity distribution. This factorization allows us to sample multiple likely $\vec{v}$ at a single $\vec{x}$ directly from $p(\vec{v}|\vec{x})$.

Flow-based solutions to the CBE were first demonstrated in simulated galaxies in [39–43], and were finally applied to real data using nearby Red Clump (w/in 4 kpc) [44] and Main Sequence (w/in 1 kpc) [45] stars from *Gaia* DR3 [46, 47]. These studies made the first fully data-driven measurements of the local gravitational potential and provided estimates of the local density of dark matter, a key input for dark matter direct detection experiments.

The present work improves on three limitations seen in [44]:

- Dust extinction introduces spatially-varying incompleteness in the observed stellar populations from *Gaia*, biasing the observed phase space density and solutions to the CBE.
- Accelerations were not continuous functions of position, and did not enforce curl-free acceleration and positive mass density constraints.
- Calculations of the mass density required computationally expensive spatial averages over large kernels, limiting the resolution of the density map.

We overcome these limitations by introducing two position-dependent functions parameterized as neural networks: the potential $\Phi(\vec{x})$, and a dust "efficiency" function $\epsilon(\vec{x})$, which we solve for directly from the equilibrium CBE using the phase space gradients from the data-driven flows.

2 Methods

2.1 Dust correction

In Ref. [48], we noted that the introduction of a position-dependent dust correction factor $\epsilon(\vec{x})$ does not introduce degeneracies with $\Phi(\vec{x})$, another unknown function of position. We define $\epsilon(\vec{x})$ through its relation to the observed phase space density $f_{\rm obs}$ (modeled by flows) and the dust-corrected phase space density f that obeys the equilibrium CBE:

$$f_{\rm obs}(\vec{x}, \vec{v}) \equiv \epsilon(\vec{x}) f(\vec{x}, \vec{v}) \tag{2}$$

where $\epsilon \approx 1$ in regions with minor dust extinction, and $\epsilon \to 0$ in regions with severe dust extinction where few Red Clump stars are observed. We write the equilibrium CBE in terms of the observed phase space density and $\epsilon(\vec{x})$:

$$\vec{v} \cdot \vec{\nabla} \ln f_{\rm obs} - \vec{v} \cdot \vec{\nabla} \ln \epsilon(\vec{x}) - \vec{\nabla}\Phi(\vec{x}) \cdot \frac{\partial \ln f_{\rm obs}}{\partial \vec{v}} = 0. \tag{3}$$

Here, ϵ has appeared in a new term coupled directly to the velocity $\vec{v}$, whereas Φ is coupled to the phase space gradient. Given sufficient information about the velocity distribution at any location $\vec{x}$ – which directly modeled by the $p(\vec{v}|\vec{x})$ flow – the degeneracy between ϵ and Φ is broken and they may be uniquely determined.

2.2 Continuum solution to the CBE

Instead of solving a system of equations for $\vec{\nabla}\Phi$, $\vec{\nabla}\epsilon$ at a single $\vec{x}$, we minimize the functional loss:

$$\mathcal{L}_{\boldsymbol{\theta},\boldsymbol{\vartheta}} = \iint d^3x d^3v f(\vec{x},\vec{v}) \left|\mathrm{CBE}(\vec{x},\vec{v})\right|^2 \tag{4}$$

to optimize for the Φ and ϵ networks as smooth functions of position. This integral form of the CBE is intractable, and is instead solved with a discrete sum over millions of collocation points in 6D space. We sample a set of $N_x = 2^{22}$ positions drawn from $n_{\mathrm{obs}}(\vec{x})$, each with $N_v = 16$ velocities drawn from $p(\vec{v}|\vec{x})$ – larger than the 6 required for the 6 unknown degrees of freedom – and sum the CBE over batches of pairs:

$$\mathcal{L}_{\boldsymbol{\theta},\boldsymbol{\vartheta}} = \frac{1}{N} \sum_{\vec{x}_i,\vec{v}_{i,j}\sim f_{\mathrm{obs}}}^{N=N_x N_v} \left(\left| \vec{v}\cdot\vec{\nabla}\ln f_{\mathrm{obs}} - \vec{\nabla}\Phi_{\boldsymbol{\vartheta}}(\vec{x}) \cdot \frac{\partial \ln f_{\mathrm{obs}}}{\partial \vec{v}} - \vec{v}\cdot\vec{\nabla}\ln\epsilon_{\boldsymbol{\theta}}(\vec{x}) \right|^2 + \mathcal{L}_{\mathrm{reg}}(\vec{x}) \right)_{\vec{x}_i,\vec{v}_{i,j}} \tag{5}$$

where $\mathcal{L}_{\mathrm{reg}}$ is the sum of the ϵ and Φ regularization terms introduced in Section 2.4. The MAFs are frozen during this training, so the $\partial_x f$ and $\partial_v f$ gradient terms at all of these collocation points can be precomputed once to rapidly evaluate Eq. 5.

2.3 Network architecture

The MAFs used to model $n_{\mathrm{obs}}(\vec{x})$ and $p(\vec{v}|\vec{x})$ are constructed with a sequence of two MADE [49] blocks with 10 hidden layers with widths of 48 nodes. To maintain numerical stability for second or higher-order gradients, we use the GINT activation function 6. Training is halted early using a patience for the validation loss using an $80\%/20\%$ training/validation split.

For stability and to estimate training variance, we ensemble 100 MAF trainings with random initializations. Additionally, we repeat the training procedure with bootstrap-resampled and measurement error-smeared copies of the training dataset to estimate statistical and measurement uncertainties.

Both the Φ and ϵ neural networks are composed of a sequence of 5 hidden layers, each 100 nodes wide, also with the GINT 6 activation for smooth higher order derivatives. The output of the ϵ network is smoothly mapped from $\mathbb{R}$ to $(0,1)$ to constrain it within its physically meaningful range.

Similar to the flows, we repeat this training procedure to robustly quantify training, statistical, and measurement uncertainties for both Φ and ϵ. The full error pipeline is outlined in Ref. [48].

GINT, the Gaussian integral activation function [48], is the integral of the Gaussian cumulative distribution function. GINT has several advantages over other smooth activation functions e.g. GELU [50] such as monotonicity and avoiding “ringing" in high-order derivatives. GINT is defined as:

$$\mathrm{GINT}(x) = \frac{1}{\sqrt{2\pi}}\left(e^{-\frac{1}{2}x^2} - 1\right) + \frac{1}{2}x\left(1 + \mathrm{erf}\left(\frac{x}{\sqrt{2}}\right)\right). \tag{6}$$

2.4 Regularization

The form of the CBE in Eq. 3 is insensitive to the scale of ϵ. While we are able to enforce $\epsilon < 1$ through a mapping, the CBE provides no direct way to enforce $\epsilon = 1$ in regions with no dust extinction. Therefore, this is enforced through an L2 regularization term added to the loss in Eq. 4.

$$\mathcal{L}_{\mathrm{reg}}(\vec{x}) \supseteq \lambda_\epsilon \left|\ln\epsilon(\vec{x})\right|^2. \tag{7}$$

This term penalizes deviation from $\epsilon = 1$ over the bulk of the 4 kpc observation volume where we expect little extinction. We set the λ_ϵ to the minimum scale where we see $\epsilon \approx 1$ in the halo, while minimizing pressure on regions with real dust extinction. We validate the accuracy of the ϵ function with a recent three-dimensional dust map [51] and find good agreement.

We are unable to directly enforce positive-definite mass densities. Therefore, we enforce this through L1 regularization and directly add negative densities as a penalty term to the loss in Eq. 4.

$$\mathcal{L}_{\rm reg}(\vec{x}) \supseteq \lambda_\Phi \max\left(0, -\nabla^2\Phi(\vec{x})\right). \tag{8}$$

The λ_Φ scale is set as large as possible until training instability is encountered while solving the CBE. We find few remaining regions with negative or near-zero mass density. Those that remain may indicate acute, spatially localized failures of the equilibrium assumption in the CBE.

3 Results

We train masked autoregressive flows (MAFs) [52] on the six-dimensional phase space coordinates $(\vec{x}, \vec{v})$ of $5,811,956$ Red Clump and Red Giant Branch stars from *Gaia* DR3 – selected for their relatively old age [53] and brightness – within 4 kpc of the solar location. The MAFs provide a high quality fit to the observed number density of stars, which includes precise modeling of the undesired dust lanes.

We plug density derivatives from the MAF model of $f_{\rm obs}$ into Eq. 3 and minimize Eq. 4 to train $\Phi(\vec{x})$ and $\epsilon(\vec{x})$ simultaneously. Given a solution for $\epsilon(\vec{x})$, we re-weight the observed number density to estimate the dust-corrected number density, revealing the unobscured disk of the Milky Way. This technique is able to recover significant amounts of information about the galactic midplane, despite extreme suppression from dust extinction in this region.

In Figure 1, we show contours of the measured potential within 4 kpc of the solar location. Even in the midplane at $z = 0$, we find excellent agreement with a standard parametric model of the Milky Way, `MilkyWayPotential2014` (abbreviated as `MWP2014`), implemented in the `galpy` [54] python code. This indicates that our dust corrected solution to the CBE has recovered a physically viable potential, even in the most dust-obscured regions of the sky.

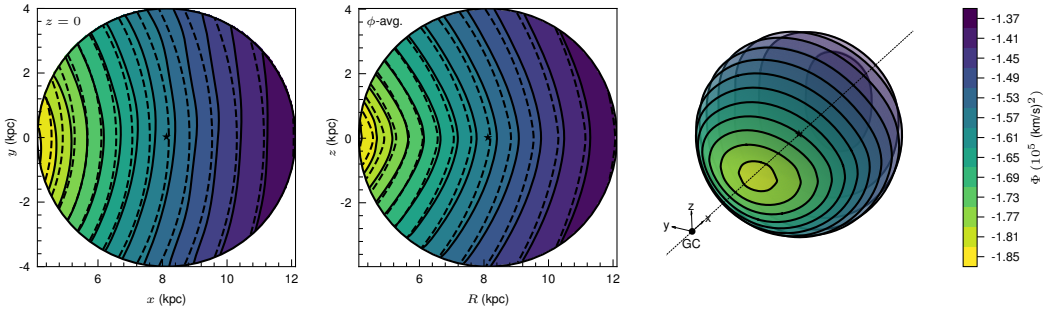

Figure 1: Left: Contours of the total gravitational potential Φ estimated in this work (solid) compared to `MWP2014` (dashed) in the midplane ($z = 0$). Middle: Azimuthally averaged Φ in the $R - z$ plane. Right: 3-dimensional isocontours of Φ within 3.8 kpc of the Solar location ($\odot$). The origin of the Galactocentric Cartesian coordinate system used in this work is placed at the Galactic Center (GC).

Next, we compute the acceleration field $\vec{a} = -\vec{\nabla}\Phi$ and visualize each component in Figure 2. Generally, we observe good agreement with `MWP2014` – particularly at the level of the vertical accelerations a_z, which is the most important term for estimating the local density – but begin to notice more nontrivial deviation in a_r and a_ϕ. Crticially, we observe significant axial acceleration, suggesting that asymmetry in the Galactic gravitational potential is causing our side of the inner Galaxy to rotate faster and the outer Galaxy to rotate slower. At the solar location, there is statistically significant but mild axial acceleration.

Finally, we compute the local mass density field ρ from Φ using Gauss's law. This yields the total mass density, whereas we are primarily interested in the distribution of dark matter. To estimate $\rho_{\rm DM}$, we subtract the baryonic component of `MWP2014`. We note that baryonic mass models are often provided without well-quantified uncertainties. To this effect, we propagate 20% errors on all parameters in the baryonic model through to the baryonic density estimate to cover the systematic variations observed across different models.

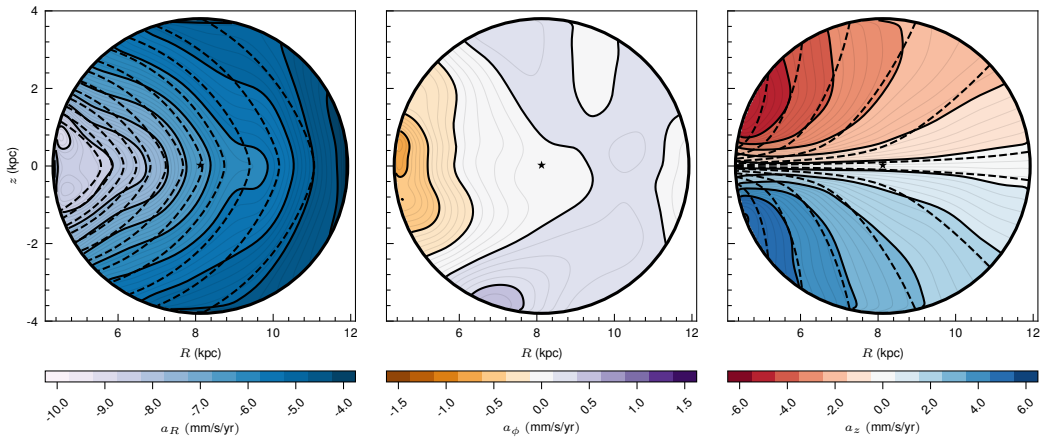

Figure 2: Azimuthally-averaged radial R (left), azimuthal ϕ (center), and vertical z (right) accelerations in the $R - z$ plane, compared to `MWP2014` (dashed).

Although noisy due to numerical second derivatives, we recover stable estimates of the local matter distribution of our Galaxy when leveraging some spatial averaging. In Figure 3, we show the azimuthally-averaged total mass density of the Galaxy along an arc at the solar radius $r_\odot = 8.122$ kpc. Dark matter halos are expected to be nearly spherically symmetric, therefore the arc of constant radius would be an "isodensity" contour for dark matter. At $s = 0$, the peak of the baryonic disk is recovered. In the tails, there is a clear, constant residual matter density not accounted for by visible matter, but which is accounted for by our dark matter halo.

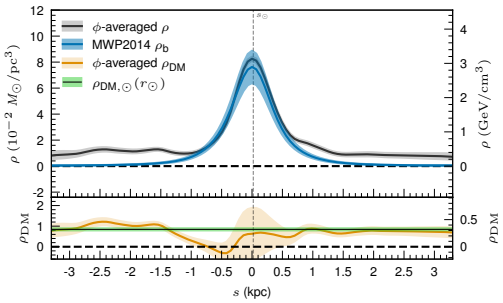

Figure 3: Azimuthally-averaged total (black) and baryonic (blue) mass density along an arc at the solar radius $r_\odot$ parametrized by $s \equiv r_\odot * (\pi/2 - \theta)$, with 1σ uncertainties shown as a band.

We find an average dark matter density at the solar radius of $\rho_{\rm DM}(r_\odot) = 0.84 \pm 0.08$ $(10^{-2}$ $\mathrm{M}_\odot/\mathrm{pc}^3) = 0.32 \pm 0.03$ $(\mathrm{GeV}/\mathrm{cm}^3)$, consistent with previous estimates of the local dark matter density [35, 37, 44, 45, 55–71].

4 Conclusion

In this paper, we introduce `ClearPotential` and apply it to the large *Gaia* DR3 astrometric dataset to measure the local gravitational potential. This approach provides a minimal-assumption, model free approach for measuring the stellar phase space of the local Galaxy and for solving the full equilibrium collisionless Boltzmann equation (CBE). We demonstrate how solutions to the CBE can be extended to automatically account for dust and position-dependent selection effects such as crowding to uncover the full unbiased phase space density and potential of the local Galaxy. Finally, we examined the consistency of this potential model with previous parametric measurements and present an estimate of the local dark matter density.

Acknowledgments and Disclosure of Funding

This work was supported by the DOE under Award Number DOE-SC0010008. The work of SHL was also partly supported by IBS under the project code, IBS-R018-D1. This work was also performed in part at Aspen Center for Physics, which is supported by National Science Foundation grant PHY-2210452. The authors acknowledge the Office of Advanced Research Computing (OARC) at Rutgers, The State University of New Jersey for providing access to the Amarel cluster and associated research computing resources that have contributed to the results reported here. URL: `https://oarc.rutgers.edu`. This research used resources of the National Energy Research Scientific Computing Center, a DOE Office of Science User Facility supported by the Office of Science of the U.S. Department of Energy under Contract No. DE-AC02-05CH11231 using NERSC award HEP-ERCAP0027491.

References

[1] V. C. Rubin, J. Ford, W. K., and N. Thonnard, Astrophys. J. **238**, 471 (1980).

[2] H. W. Babcock, Lick Observatory Bulletin **498**, 41 (1939).

[3] P. Salucci, Astron. Astrophys. Rev. **27**, 2 (2019), arXiv:1811.08843 [astro-ph.GA] .

[4] S. W. Allen, A. E. Evrard, and A. B. Mantz, Annual Review of Astronomy and Astrophysics **49**, 409 (2011), arXiv:1103.4829 [astro-ph.CO] .

[5] F. Zwicky, Helvetica Physica Acta **6**, 110 (1933).

[6] N. Aghanim *et al.* (Planck), Astronomy & Astrophysics **641**, A6 (2020), [Erratum: Astron.Astrophys. 652, C4 (2021)], arXiv:1807.06209 [astro-ph.CO] .

[7] D. Clowe, A. Gonzalez, and M. Markevitch, Astrophys. J. **604**, 596 (2004), arXiv:astro-ph/0312273 .

[8] M. R. Buckley and A. H. G. Peter, Phys. Rept. **761**, 1 (2018), arXiv:1712.06615 [astro-ph.CO] .

[9] A. Burkert, ApJ **534**, L143 (2000), arXiv:astro-ph/0002409 [astro-ph] .

[10] C. S. Kochanek and M. White, ApJ **543**, 514 (2000), arXiv:astro-ph/0003483 [astro-ph] .

[11] N. Yoshida, V. Springel, S. D. M. White, and G. Tormen, ApJ **544**, L87 (2000), arXiv:astro-ph/0006134 [astro-ph] .

[12] R. Davé, D. N. Spergel, P. J. Steinhardt, and B. D. Wandelt, ApJ **547**, 574 (2001), arXiv:astro-ph/0006218 [astro-ph] .

[13] P. Colín, V. Avila-Reese, O. Valenzuela, and C. Firmani, ApJ **581**, 777 (2002), arXiv:astro-ph/0205322 [astro-ph] .

[14] J. Koda and P. R. Shapiro, MNRAS **415**, 1125 (2011), arXiv:1101.3097 [astro-ph.CO] .

[15] M. Vogelsberger, J. Zavala, and A. Loeb, MNRAS **423**, 3740 (2012), arXiv:1201.5892 [astro-ph.CO] .

[16] M. Rocha, A. H. G. Peter, J. S. Bullock, M. Kaplinghat, S. Garrison-Kimmel, J. Oñorbe, and L. A. Moustakas, MNRAS **430**, 81 (2013), arXiv:1208.3025 [astro-ph.CO] .

[17] A. H. G. Peter, M. Rocha, J. S. Bullock, and M. Kaplinghat, MNRAS **430**, 105 (2013), arXiv:1208.3026 [astro-ph.CO] .

[18] J. Zavala, M. Vogelsberger, and M. G. Walker, MNRAS **431**, L20 (2013), arXiv:1211.6426 [astro-ph.CO] .

[19] O. D. Elbert, J. S. Bullock, M. Kaplinghat, S. Garrison-Kimmel, A. S. Graus, and M. Rocha, ApJ **853**, 109 (2018), arXiv:1609.08626 [astro-ph.GA] .

[20] E. S. Levine, L. Blitz, and C. Heiles, ApJ **643**, 881 (2006), arXiv:astro-ph/0601697 [astro-ph] .

[21] I. Minchev, A. C. Quillen, M. Williams, K. C. Freeman, J. Nordhaus, A. Siebert, and O. Bienaymé, MNRAS **396**, L56 (2009), arXiv:0902.1531 [astro-ph.GA] .

[22] S. Chakrabarti and L. Blitz, MNRAS **399**, L118 (2009), arXiv:0812.0821 [astro-ph] .

[23] C. W. Purcell, J. S. Bullock, E. J. Tollerud, M. Rocha, and S. Chakrabarti, Nature **477**, 301 (2011), arXiv:1109.2918 [astro-ph.GA] .

[24] L. M. Widrow, S. Gardner, B. Yanny, S. Dodelson, and H.-Y. Chen, ApJ **750**, L41 (2012), arXiv:1203.6861 [astro-ph.GA] .

[25] J. Bland-Hawthorn and O. Gerhard, ARA&A **54**, 529 (2016), arXiv:1602.07702 [astro-ph.GA] .

[26] J. P. Vallée, The Astronomical Review **13**, 113 (2017), arXiv:1711.05228 [astro-ph.GA] .

[27] T. Antoja, A. Helmi, M. Romero-Gómez, D. Katz, C. Babusiaux, R. Drimmel, D. W. Evans, F. Figueras, E. Poggio, C. Reylé, A. C. Robin, G. Seabroke, and C. Soubiran, Nature **561**, 360 (2018), arXiv:1804.10196 [astro-ph.GA] .

[28] A. Helmi, C. Babusiaux, H. H. Koppelman, D. Massari, J. Veljanoski, and A. G. A. Brown, Nature **563**, 85 (2018), arXiv:1806.06038 [astro-ph.GA] .

[29] S. Chakrabarti, P. Chang, A. M. Price-Whelan, J. Read, L. Blitz, and L. Hernquist, ApJ **886**, 67 (2019), arXiv:1906.04203 [astro-ph.GA] .

[30] A.-C. Eilers, D. W. Hogg, H.-W. Rix, N. Frankel, J. A. S. Hunt, J.-B. Fouvry, and T. Buck, ApJ **900**, 186 (2020), arXiv:2003.01132 [astro-ph.GA] .

[31] J. Shen and X.-W. Zheng, Research in Astronomy and Astrophysics **20**, 159 (2020), arXiv:2012.10130 [astro-ph.GA] .

[32] J. A. S. Hunt and E. Vasiliev, New A Rev. **100**, 101721 (2025), arXiv:2501.04075 [astro-ph.GA] .

[33] S. Sivertsson, H. Silverwood, J. I. Read, G. Bertone, and P. Steger, Monthly Notices of the Royal Astronomical Society **478**, 1677 (2018), arXiv:1708.07836 [astro-ph.GA] .

[34] J.-B. Salomon, O. Bienaymé, C. Reylé, A. C. Robin, and B. Famaey, Astronomy & Astrophysics **643**, A75 (2020), arXiv:2009.04495 [astro-ph.GA] .

[35] M. S. Nitschai, M. Cappellari, and N. Neumayer, Monthly Notices of the Royal Astronomical Society **494**, 6001 (2020), arXiv:1909.05269 [astro-ph.GA] .

[36] M. S. Nitschai, A.-C. Eilers, N. Neumayer, M. Cappellari, and H.-W. Rix, Astrophys. J. **916**, 112 (2021), arXiv:2106.05286 [astro-ph.GA] .

[37] R. Guo, C. Liu, S. Mao, X.-X. Xue, R. J. Long, and L. Zhang, Monthly Notices of the Royal Astronomical Society **495**, 4828 (2020), arXiv:2005.12018 [astro-ph.GA] .

[38] J. H. J. Hagen and A. Helmi, Astronomy & Astrophysics **615**, A99 (2018), arXiv:1802.09291 [astro-ph.GA] .

[39] G. M. Green, Y.-S. Ting, and H. Kamdar, ApJ **942**, 26 (2023), arXiv:2205.02244 [astro-ph.GA] .

[40] J. An, A. P. Naik, N. W. Evans, and C. Burrage, Monthly Notices of the Royal Astronomical Society **506**, 5721 (2021), arXiv:2106.05981 [astro-ph.GA] .

[41] A. P. Naik, J. An, C. Burrage, and N. W. Evans, Monthly Notices of the Royal Astronomical Society **511**, 1609 (2022), https://academic.oup.com/mnras/article-pdf/511/2/1609/48413075/stac153.pdf .

[42] M. R. Buckley, S. H. Lim, E. Putney, and D. Shih, MNRAS **521**, 5100 (2023), arXiv:2205.01129 [astro-ph.GA] .

[43] T. Kalda, G. M. Green, and S. Ghosh, MNRAS **527**, 12284 (2024), arXiv:2310.00040 [astro-ph.GA] .

[44] S. H. Lim, E. Putney, M. R. Buckley, and D. Shih, J. Cosmology Astropart. Phys. **2025**, 021 (2025), arXiv:2305.13358 [astro-ph.GA] .

[45] T. Kalda and G. M. Green, arXiv e-prints , arXiv:2507.03742 (2025), arXiv:2507.03742 [astro-ph.GA] .

[46] L. Lindegren, S. A. Klioner, J. Hernández, A. Bombrun, M. Ramos-Lerate, H. Steidelmüller, U. Bastian, M. Biermann, A. de Torres, E. Gerlach, R. Geyer, T. Hilger, D. Hobbs, and et al., Astronomy & Astrophysics **649**, A2 (2021).

[47] Gaia Collaboration, A. Vallenari, A. G. A. Brown, T. Prusti, and J. H. J. e. a. de Bruijne, arXiv e-prints , arXiv:2208.00211 (2022), arXiv:2208.00211 [astro-ph.GA] .

[48] E. Putney, D. Shih, S. H. Lim, and M. R. Buckley, arXiv e-prints , arXiv:2412.14236 (2024), arXiv:2412.14236 [astro-ph.GA] .

[49] M. Germain, K. Gregor, I. Murray, and H. Larochelle, in *Proceedings of the 32nd International Conference on Machine Learning*, Proceedings of Machine Learning Research, Vol. 37, edited by F. Bach and D. Blei (PMLR, Lille, France, 2015) pp. 881–889.

[50] D. Hendrycks and K. Gimpel, arXiv e-prints (2016), arXiv:1606.08415 [cs.LG] .

[51] R. Lallement, J. L. Vergely, C. Babusiaux, and N. L. J. Cox, A&A **661**, A147 (2022), arXiv:2203.01627 [astro-ph.GA] .

[52] G. Papamakarios, T. Pavlakou, and I. Murray, in *Advances in Neural Information Processing Systems*, Vol. 30, edited by I. Guyon, U. V. Luxburg, S. Bengio, H. Wallach, R. Fergus, S. Vishwanathan, and R. Garnett (Curran Associates, Inc., 2017) arXiv:1705.07057 [stat.ML] .

[53] L. Girardi, ARA&A **54**, 95 (2016).

[54] J. Bovy, ApJS **216**, 29 (2015), arXiv:1412.3451 [astro-ph.GA] .

[55] J. Buch, S. C. J. Leung, and J. Fan, JCAP **04**, 026 (2019), arXiv:1808.05603 [astro-ph.GA] .

[56] K. Schutz, T. Lin, B. R. Safdi, and C.-L. Wu, Phys. Rev. Lett. **121**, 081101 (2018), arXiv:1711.03103 [astro-ph.GA] .

[57] M. D. Wardana, H. Wulandari, Sulistiyowati, and A. H. Khatami, in *European Physical Journal Web of Conferences*, European Physical Journal Web of Conferences, Vol. 240 (2020) p. 04002.

[58] O. Bienaymé, A. C. Robin, J. B. Salomon, and C. Reylé, arXiv e-prints , arXiv:2406.08158 (2024), arXiv:2406.08158 [astro-ph.GA] .

[59] R. Guo, J. Shen, Z.-Y. Li, C. Liu, and S. Mao, ApJ **936**, 103 (2022), arXiv:2208.03667 [astro-ph.GA] .

[60] A. Widmark, C. F. P. Laporte, P. F. de Salas, and G. Monari, A&A **653**, A86 (2021), arXiv:2105.14030 [astro-ph.GA] .

[61] C. Wegg, O. Gerhard, and M. Bieth, Monthly Notices of the Royal Astronomical Society **485**, 3296 (2019), arXiv:1806.09635 [astro-ph.GA] .

[62] K. Hattori, M. Valluri, and E. Vasiliev, Monthly Notices of the Royal Astronomical Society **508**, 5468 (2021), arXiv:2012.03908 [astro-ph.GA] .

[63] M. Cautun, A. Benítez-Llambay, A. J. Deason, C. S. Frenk, A. Fattahi, F. A. Gómez, R. J. J. Grand, K. A. Oman, J. F. Navarro, and C. M. Simpson, MNRAS **494**, 4291 (2020), arXiv:1911.04557 [astro-ph.GA] .

[64] P. J. McMillan, MNRAS **465**, 76 (2017), arXiv:1608.00971 [astro-ph.GA] .

[65] Y. Zhou, X. Li, Y. Huang, and H. Zhang, arXiv e-prints , arXiv:2212.10393 (2022), arXiv:2212.10393 [astro-ph.GA] .

[66] Y. Sofue, Galaxies **8**, 37 (2020), arXiv:2004.11688 [astro-ph.GA] .

[67] I. Ablimit, G. Zhao, C. Flynn, and S. A. Bird, The Astrophysical Journal Letters **895**, L12 (2020).

[68] P. F. de Salas, K. Malhan, K. Freese, K. Hattori, and M. Valluri, J. Cosmology Astropart. Phys. **2019**, 037 (2019), arXiv:1906.06133 [astro-ph.GA] .

[69] Y. Huang, X. W. Liu, H. B. Yuan, M. S. Xiang, and H. W. e. a. Zhang, MNRAS **463**, 2623 (2016), arXiv:1604.01216 [astro-ph.GA] .

[70] M. Pato, F. Iocco, and G. Bertone, J. Cosmology Astropart. Phys. **2015**, 001 (2015), arXiv:1504.06324 [astro-ph.GA] .

[71] L. Casagrande, ApJ **896**, 26 (2020), arXiv:2005.09131 [astro-ph.GA] .